Available online at www.sciencedirect.com
ScienceDirect
Geochimica et Cosmochimica Acta 71 (2007) 5339–5354
Geochimica et Cosmochimica Acta
www.elsevier.com/locate/gca

Temporal variations of colloidal carrier phases and associated trace elements in a boreal river

Ralf Dahlqvist [a,b,*], Karen Andersson [d,1], Johan Ingri [c], Tobias Larsson [d], Björn Stolpe [d], David Turner [d]

[a] Department of Geology and Geochemistry, Stockholm University, SE-106 91 Stockholm, Sweden
[b] Laboratory for Isotope Geology, Swedish Museum of Natural History, Box 50007, SE-104 05 Stockholm, Sweden
[c] Division of Applied Geology, Luleå University of Technology, SE-971 87 Luleå, Sweden
[d] Marine Chemistry, Department of Chemistry, Göteborg University, SE-412 96 Göteborg, Sweden

Received 9 January 2007; accepted in revised form 18 September 2007; available online 29 September 2007

Abstract

Elemental size distributions, from truly dissolved through colloidal to particulate, have been studied in a subarctic boreal river. The measurements, carried out during 2002, ranged from winter to summer conditions, including an intense spring flood event. Results are reported for a total of 42 elements. Size distributions were characterised using a combination of cross-flow (ultra)filtration (CFF), flow field-flow fractionation (FlFFF), and diffusive gradients in thin-films (DGT). The three techniques showed similar trends, but quantitative comparisons reveal some important differences that warrant further investigation.

Previous work has identified two colloidal carrier phases in fresh waters, dominated by iron and carbon, respectively. The majority of the elements studied are associated with one or both of these colloidal carrier phases. The exceptions are the alkali metals and several anions that are only very weakly associated with colloidal material, and which therefore occur mainly as truly dissolved material (<1 kDa in molecular weight). We discuss the likely origin for the two colloidal carrier phases and consider how associated trace elements fit into the geochemical framework. The relative affinities of the elements for iron and carbon colloidal carrier phases are related to their chemistries, and are compared with earlier data from the Delsjö Creek in southern Sweden.

Elemental colloidal concentrations show strong seasonal variations related to changes in the colloidal carrier phase(s) with which they associate. In particular, many elements show a strong spring maximum in colloidal concentrations associated with the strong maximum in colloidal carbon concentration during the spring flood.

1. INTRODUCTION

Assessment of colloidal material presents a series of challenges to the aquatic geochemist: it covers a wide size range (nominally 1 nm–1 μm), and is chemically and physically heterogeneous (Gustafsson and Gschwend, 1997). Despite significant methodological advances in recent years, no method for physico-chemical fractionation in the colloidal size range is without potential artifacts. It is therefore advantageous to use several different methods in parallel, in order to minimize the risk of interpreting artifacts as natural variations (Buffle et al., 1998).

Along with aeolian dust, a major input of trace elements to the ocean is through river discharge. The fate of trace elements in estuarine processes and in the ocean is largely dependent on how the elements are associated to particles and colloids, and/or are present as dissolved species. These characteristics are shaped during terrestrial low tempera-

* Corresponding author. Present Address: Oxford University, Department of Earth Sciences, Parks Road, Oxford OX1 3PR, UK. Fax: +44 1865 272072.
E-mail address: Ralf.Dahlqvist@earth.ox.ac.uk (R. Dahlqvist).
[1] To be contacted via David Turner.

0016-7037/$ - see front matter © 2007 Elsevier Ltd. All rights reserved.
doi:10.1016/j.gca.2007.09.016

ture geochemical processes in fresh water solutions, carrying solute species and colloidal and particulate material. Hence, the study of trace elements and their physicochemical properties in fresh water systems, such as rivers, is important for understanding their fate in the ocean.

The major annual hydrological event for rivers located in the boreal and arctic zones is snowmelt in spring, which causes a dramatic increase in discharge. For instance, most rivers at this latitude draining their water to the Arctic Ocean deliver 40–80% of the annual volume during the spring flood (Arnborg et al., 1967; Gordeev et al., 1996). The load of total suspended matter, organic carbon, and major and trace elements often show large variations in concentration during this episode (e.g. Rember and Trefry, 2004; Ingri et al., 2005; Neff et al., 2006), which not only indicates the importance of performing temporal scale studies with frequent sampling to cover seasonal variations, but also that there still remains much to learn about the nature of the matter transported in river water during such changing conditions.

The studied river, Kalix River, is in many aspects similar to several Russian rivers. It represents an unregulated pristine medium-sized boreal river, draining a till-covered bedrock with mainly granitic origin, and has previously been well characterized in several studies of major and trace elements and isotopes (Pontér et al., 1990; Öhlander et al., 1991, 1996, 2000; Ingri and Widerlund, 1994; Ingri et al., 1997, 2000, 2005, 2006; Porcelli et al., 1997; Land and Öhlander, 1997; Andersson et al., 1998, 2001; Land et al., 1999, 2000a,b; Dahlqivst et al., 2004, 2005). It has been indicated that temporal variations in river runoff is highly correlated to different hydro-geological pathways; a topic which has been highlighted by e.g. Andersson et al. (2006), Neff et al. (2006) and Pokrovsky et al. (2006). Thus, intensity and duration of precipitation and/or snowmelt episodes will control residence times and pathways for soil and ground water, and so have a direct influence on the geochemical imprint of river water, including the chemical composition of the colloidal material.

Arctic and boreal regions holds some of the most important reservoirs for organic carbon (Post et al., 1982; Botch et al., 1995). Peatlands along with organic-rich soils are common features of the boreal and arctic regions on the Eurasian and North-American continents. An increasing global warming at high latitudes in the boreal and arctic zones will most likely change both the amount and character of released organic carbon, including the colloidal fraction. In turn, the changes are likely to also affect transport of elements associated to the released organic material.

The chemical composition and concentration of colloidal particles in river water seems to be a highly variable and affected by variations in hydro-geological pathways. Two different colloidal phases have been identified in recent publications. In Dahlqivst et al. (2004) and Andersson et al. (2006) direct measurements showed the presence of two different colloidal carrier phases; one organic-rich and another Fe-rich component. These two carrier phases were also distinctly different in size. A study in a southern Swedish creek also identified the same two carrier phases in the colloidal size range (Lyvén et al., 2003).

Another study identifying specific colloidal particles is Allard et al. (2004), where spectroscopic and microscopic techniques were applied to characterize Fe-rich colloidal matter in Amazonian rivers. However, direct measurements of the chemistry and size of colloidal particles are rare, and studies on temporal variations of these are even more scarce.

In this paper, we present major and trace element data obtained using several techniques for physicochemical characterization of sampled species, ranging in size from diffusible ions to particles $<100\ \mu m$. The study show the temporal variation of 42 elements in these fractions from winter conditions, through a distinct spring flood event, and into summer conditions, with focus on assessing the colloidal chemistry and size distribution. The colloidal carrier phases previously identified in the Kalix River (Dahlqivst et al., 2004; Andersson et al., 2006) are used to categorize the trace elemental composition and deduce a likely source for the colloidal material.

The methods used during the study include Cross-Flow (ultra)Filtration (CFF), Flow Field-Flow Fractionation coupled on-line to Inductively Coupled Plasma – Mass Spectrometry (FlFFF-ICP-MS), and Diffusive Gradients in Thin films (DGT). Each of these techniques has limitations regarding resolution in size and/or other operational restraints. However, in many respects they complement each other. Using them together provide more detailed information for interpretation of speciation/fractionation data, and a welcome opportunity to critically assess the data and to identify possible artifacts.

A detailed chemical and physical description of aqueous colloids and particles in terrestrial surface and ground waters may be of great relevance for future studies in the light of global climate change and warming. Changing climatic conditions are likely to significantly affect annual mean temperatures in the boreal and arctic regions and modify both type and amount of precipitation, thus directly affecting hydro-geological pathways. A longer growth period for terrestrial plants will enhance organic production and cycling and possibly increase the reservoir of organic carbon in soils, which is a likely source for organic colloids in surface waters. At the same time thawing permafrost will release large quantities of organic carbon to stream waters. It is difficult to assess how global climatic changes will affect regional hydro-geochemistry. It can be argued that ground waters with long residence times are sources for surface waters with high concentrations of Fe-rich colloids. In contrast to this are soil waters rapidly washing the uppermost organic-rich layers, e.g. during episodes of intense snowmelt or rainstorms, acting as a source for organic-rich colloids. However, it is clear that the colloidal fraction will continue to be a significant component in surface waters and a carrier for other trace elements. It is therefore important to understand current processes and conditions under which certain types of colloids are present and of significance for the total transport of major and trace elements from the terrestrial environment to the ocean.

2. METHODS

The sampling and analysis protocols used are essentially the same as those reported in connection with the discussion of lanthanide chemistry in the ''Kalix 2002'' project (Andersson et al., 2006), although there are some differences in the treatment of the DGT results.

2.1. Sampling area

The Kalix River in northern Sweden is part of a pristine river system, which also includes the Torne River (Dynesius and Nilsson, 1994); no man-made dams or other constructions influence the water discharge. A map of the catchment can be found in Andersson et al. (2006) The mean annual discharge is 296 $m^3 s^{-1}$, with low flows below 100 $m^3 s^{-1}$ during winter, and high flows up to 1600 $m^3 s^{-1}$ during the spring flood. The drainage area is $\sim 2.4 \times 10^4$ km^2 and stretches from the Scandinavian part of the Caledonian mountain range in the northwest to the Gulf of Bothnia. About 60% of the water in the nearby Torne River drains via a bifurcation into the Kalix River, and together these two rivers constitute the largest unregulated river system in northern Europe.

The basement in the catchment can be divided into two different areas. The Caledonides in the northwest cover about 5% of the basement and mainly consists of mica schist, quartzite and amphibolite (Gee and Zachrisson, 1979). The remaining part of the basement is Precambrian bedrock of granitic composition, with features of acidic, intermediate and basic volcanic rocks along with sedimentary rocks, more or less affected by metamorphism (Gaal and Gorbatschev, 1987). The quaternary cover is dominated by till deposited during the last glacial period. The till has a well-developed podzol profile (Fromm, 1965). Coniferous forests of spruce and pine cover 55–65% of the catchment area, and peatland about 20%: farmland accounts for no more than 1%. Some post-glacial sediments are deposited close to the river and its contributors. Mean annual temperature and precipitation are ~0.2 °C and ~500 mm, respectively.

Because of its northerly geographical location at the Arctic Circle, the river is covered by ice from the end of November to April. Throughout this period precipitation is accumulated as snow in the catchment. Hence, the geochemistry of Kalix River water is mainly controlled by inflow of groundwater during winter base-flow. The melting period usually starts in late April or early May, and peak discharge generally occurs in mid-May. During peak discharge the pH drops, and concentrations of TOC and Fe increase, while major elements like Na, K, Ca, Mg, Cl, SO_4 and HCO_3 are diluted by melt water.

2.2. Water sampling

Sampling was performed in the Kamlunge rapids from January to June 2002. The sampling station is located about 30 km upstream from the river mouth. Water samples (50 L) were prefiltered in the field with a 100 μm nylon mesh filter mounted in a 142 mm in-line acrylic filter holder (Geotech®, Denver, CO, USA), and collected in two 25 L polyethylene (PE) carboys. The three exceptions to this are the samples collected in January (25 L sample) and February, when no prefiltration was performed, and March when a 25 μm membrane filter cartridge was used for prefiltration. River water was flushed through the system for a few minutes before any sample was collected. The carboys containing the prefiltered water were thereafter transported to the laboratory where CFF and FlFFF processing commenced. All equipment, i.e. filter holder, nylon mesh, tubing and carboys, was acid-cleaned in 5% HNO_3 for at least 48 h and rinsed in ultrapure, Milli-Q® (MQ, Millipore, Billerica, MA, USA), water (>18 MΩ cm) prior to use.

Water temperature, pH and conductivity were monitored in the field during sampling either with a Mini-Sonde®3 or a DataSonde®4a (Hydrolab, Loveland, CO, USA). The instruments were calibrated prior to each sampling, and data was collected for at least 30 min. pH was measured to ±0.01 pH unit (1 s.d.). Prefiltered samples were also collected and analyzed for total organic carbon (TOC) and fluorescence.

2.3. DGT-sampling

The in situ speciation method of Diffusive Gradients in Thin films (DGT) (Davison and Zhang, 1994; Davison et al., 2000) was used to sample the labile fraction of metals in the Kalix River. The DGT devices were made and prepared for sampling by following the procedure described by Davison et al. (2000).

DGT-sampling was performed on 9 occasions from January to June 2002. Triplicate DGT devices were deployed in the rapids on each occasion, and deployment times ranged from 120 to 215 h. The deployment time for each sampling occasion was determined, and a temperature-logging device (Onset® StowAway TidbiT™, Bourne MA, USA) was deployed together with the DGT devices to monitor the water temperature. This temperature monitoring is performed in order to calculate diffusion coefficients for the metal ions in the water. Directly upon retrieval in the field, the DGT devices were thoroughly rinsed in MQ water and placed in airtight PE plastic bags. Several barriers of plastic were used to avoid contamination. The DGT devices were prepared for analysis according to Dahlqvist et al. (2002) and analyzed using ICP-MS.

The mass of metal X accumulated in a DGT sampler has previously been used to calculate labile metal concentrations using Fick's first law of diffusion according to Davison and Zhang (1994),

$$[\mathrm{X}]_{\mathrm{labile}} = \frac{M_{\mathrm{X}} \Delta g}{D_{\mathrm{X}} A t} \quad (1)$$

where M_X is the total mass of the metal X accumulated in the DGT sampler and analyzed in the elution acid, Δg is the thickness of the diffusion layer (set equal to the gel thickness), D_X is the diffusion coefficient for the metal X in acrylamide hydrogel, A is the area exposed by a DGT device to the solution, and t is the deployment time. Values of D_X for free metal ions in water at 25 °C were taken from Vanýsek

(2005), and were corrected to the mean in situ sampling temperature using the Stokes–Einstein relation,

$$\frac{D_1\eta_1}{T_1} = \frac{D_2\eta_2}{T_2} \quad (2)$$

where D_i and η_i and are the diffusion coefficient and water viscosity respectively at two different temperatures T_1 and T_2 (kelvin). A recent study of the diffusion of Pb^{2+}, Ni^{2+}, Cd^{2+} and Cu^{2+} shows that diffusion coefficients in acrylamide hydrogel at low ionic strength (1 mM) are 90% of the corresponding values in pure water (Scally et al., 2006): the diffusion coefficients calculated according to Eq. 2 were therefore further corrected by the factor 0.9.

The use of Eq. 1 to calculate labile metal concentrations assumes that the species diffusing through the gel is the free metal ion. However, it has recently been shown that larger entities such as metal-fulvic acid complexes can diffuse through the gel, albeit with significantly lower diffusion coefficients (Scally et al., 2006). The interpretation of the DGT measurements in the light of this observation is discussed in Section 3.4.

2.4. CFF

Ultrafiltration is used to collect and enrich suspended colloids in a retentate solution for analysis. The technique is based on the assumption that only colloids larger than the pore size of the ultrafiltration membrane are enriched, and that the matrix of permeable species remain unaltered. However, previous work suggests that permeable species also are affected by retention (e.g. Viers et al., 1997; Guo et al., 2001; Dahlqivst et al., 2004).

The normal method for calculating the concentration of the colloidal or particulate fraction is to use concentrations measured in the retentate and permeate fractions.

$$[X]_{\text{Coll./Part.}} = \frac{[X]_{\text{Ret}} - [X]_{\text{Perm}}}{\text{c.f.}} \quad (3)$$

where c.f. is the concentration factor.

$$\text{c.f.} = \frac{\text{Vol.}_{\text{Ret}} + \text{Vol}_{\text{Perm}}}{\text{Vol.}_{\text{Ret}}} \quad (4)$$

The sampling and analysis setup used during this study is presented in detail in Andersson et al. (2006). No samples were drawn from the permeate or retentate lines during progress of ultrafiltration. Integrated samples of permeate and retentate were collected after completed ultrafiltration. A Millipore Pellicon®2 acrylic filter holder and a high performance peristaltic Watson Marlow® pump were used. Four types of Millipore Cassette® filters (0.46 m^2) were used: 0.22 μm, 10 and 1 kDa. Da (Dalton) is equivalent to the unified atomic mass unit. A pore size of 1 kDa is roughly equivalent to a size of 1 nm, and 10 kDa to 5 nm, the exact relationship depending on the three-dimensional structure of the colloids in question. On one occasion a 1 MDa filter was used as substitute for the 0.22 μm filter (May 6): the May 6 data should therefore be interpreted with caution since the relative performance of these two filter membranes has not been assessed. The membrane materials were polyvinylidene fluoride (PVDF) for the 0.22 μm filter, and regenerated cellulose for the 1 MDa, 10 kDa and 1 kDa filters. Ultrafiltration settings are summarized in Table 1.

The filters were first rinsed with large amounts of MQ water to remove the organic storage solution. A complete cleaning cycle was performed with basic and acidic solutions according to the specifications given by the manufacturer. These solutions were prepared from MQ water, p.a. (analytical grade) NaOH and p.a. HCl. The filters were thoroughly rinsed with MQ water between the base and acid solutions and after the acid solution. In all, each filter was rinsed with about 100 L of ultrapure solution prior to use. Each filter was preconditioned with about 2 L of sample solution before starting the actual filtration. A new cleaning cycle using NaOH and HCl was then performed before the processing of each new sample. Cleaned filters were stored in airtight plastic bags in the dark at ~5 °C between filtrations.

The collected water samples (50 L) were immediately ultrafiltered with the 0.22 μm filter upon arrival to the laboratory. The retentate solution was reduced to about 3 L before closing the permeate line. The permeate fraction was collected in clean 25 L PE carboys.

A small volume (<2 L) of the 0.22 μm permeate was analyzed by FlFFF-HR ICP-MS (see Section 2.5), and equal volumes of the remaining 0.22 μm permeate were used for ultrafiltration with the 10 kDa and 1 kDa filters, respectively. The volume of the retentate solutions from the 10 and 1 kDa filtrations were reduced to 1.5–2.0 L. Trace metal concentrations were determined by ICP-MS for all retentate and permeate solutions.

All ultrafiltrations (0.22 μm, 10 kDa and 1 kDa) were completed within 14 h of sample collection. During all ultrafiltrations the retentate volume was kept constant at ~4 L until the end of each filtration, when the volume was reduced. This was achieved by continuously transferring feed solution from the 25 L carboy to a 5 L retentate flask at the same rate as the permeate flow. At the end of each filtration, the retentate solution was allowed to circulate through the system with the permeate line closed for

Table 1
Ultrafiltration settings during the Kalix 2002 project

Filter typeand cut-off	Membranematerial	Retentate flow (L min^{-1})	Permeate flow (mL min^{-1})	Crossflow ratio	Average c.f.[a]
Double 0.22 μm	PVDF	7.8	250	31	16.1
Single 10 kDa	Regenerated cellulose	5.5	250	22	10.9
Double 1 kDa	Regenerated cellulose	4.0	75	53	9.6
Single 1 MDa[b]	Regenerated cellulose	4.8	250	19	16.9

[a] c.f. = concentration factor.
[b] Used once on May 6 as replacement for 0.22 μm filter.

10 min as recommended by Benner (1991) for improved recoveries. All retentates, permeates and the prefiltered sample were analyzed for elemental concentrations with ICP-MS (ELEMENT®, Thermo Finnigan) according to Long and Martin (1990). Typical measurement uncertainties (1 s.d.) for key elements are <4% (Fe), <12% (Al), <10% (Co), <9% (Mo), <5% (Ni) and <3% (Rb). The settings used during ultrafiltration, including membrane material, retentate and permeate flows are presented in Andersson et al. (2006). Average recoveries were calculated as the amount of an element present in the permeate and retentate solutions divided by the total amount in the feed solution:

$$\text{Rec.} = \frac{\text{Vol.}_{\text{Ret}}[\text{X}]_{\text{Ret}} + \text{Vol.}_{\text{Perm}}[\text{X}]_{\text{Perm}}}{\text{Vol.}_{\text{Feed}}[\text{X}]_{\text{Feed}}} \quad (5)$$

Recoveries for the 0.22 μm ultrafilter were: 0.36 (Fe), 0.96 (OC), 0.45 (Al), 0.73 (Co), 0.93 (Mo), 0.84 (Ni) and 0.99 (Rb). For the other two filters recoveries for these elements were: 0.74, 0.68, 0.77, 0.77, 0.89, 0.91 and 0.92 (10 kDa), and 0.86, 0.83, 0.84, 0.72, 0.95, 0.92, 0.98 (1 kDa). The low recoveries for some elements with the 0.22 μm ultrafilter, most notably Fe, indicate that Fe colloids or particles may strongly interact with the membrane surface. Either the size range of the colloidal/particulate matter is unfavourable for use with this particular membrane, or the membrane interacts electrostatically with the colloids.

2.5. FlFFF-ICP-MS

Field-flow fractionation (FFF) is a family of chromatography-like techniques by which continuous size distributions of colloidal material can be determined quantitatively. Flow FFF is the most suitable FFF technique for studying small (1–50 nm) natural aquatic colloids. The sample is eluted through a thin, flat channel by a laminar hydrodynamic flow (the channel flow). A second flow (the cross flow) is applied perpendicular to the channel flow, forcing the sample colloids towards the lower (accumulation) wall of the FlFFF channel. An ultrafilter membrane covers the accumulation wall. Thus, colloids larger than the cutoff size are retained in the channel, while the dissolved fraction permeates through the membrane. The average position of a colloid in the channel will depend on its ability to diffuse against the cross flow. In this setup, smaller colloids are transported faster in the parabolic channel flow and elute first from the FlFFF channel. Since the fractionation is based on simple physical properties, which can be theoretically described, the diffusion coefficient—and hence the hydrodynamic diameter—can be calculated directly from the retention time and the channel dimensions (Giddings et al., 1976). The relation between retention time and relative molar mass can also be determined by calibration with polymer standards of known relative molar mass (Beckett et al., 1987).

A detailed description of the principles and operating procedure of the system used in the 'Kalix 2002' project is described in Hassellöv et al. (1999). The system is made up of a size-separating unit (FlFFF) followed by three on-line detectors in series (a flow-through UV detector measuring organic carbon, a flow-through fluorescence detector measuring humic material, and a High Resolution ICP-MS quantifying elemental concentrations) as shown in Andersson et al. (2006). This allows determination of elemental composition as a function of colloid size in a measurement time of 100 min. A quantitative on-channel pre-concentration procedure was used to enable the injection of a sample volume of 45 mL (Lyvén et al., 1997).

Modifications of the method compared to Hassellöv et al. (1999) include the use of a HR ICP-MS (ELEMENT®, Thermo Finnigan) instead of a quadrupole ICP-MS, and a different FlFFF carrier solution (15 mM NH_4NO_3, pH 7.0). The FlFFF carrier was optimized to resemble the natural chemical environment and to be compatible with the demands of both the FlFFF separation and the ICP-MS with respect to ionic strength and pH. The operating conditions for the setup are listed in Table 2, and detection limits for FlFFF-ICP-MS are described in Stolpe et al. (2005).

The signals obtained from the ICP-MS were converted to elemental concentrations using blanks and standards prepared in the same matrix as the sample (NH_4NO_3) and with 1% (v/v) nitric acid. The 'concentration vs. retention time'-curve, referred to as a fractogram, was integrated to give the total peak area. The area was then converted to amount of element by multiplication of the flow rate and the dilution factor in the FFF-ICP-MS interface. This amount was then compared with the total amount injected (sample volume multiplied by filtered total sample concentration). The total filtered sample concentration was determined by measuring an acidified filtered sample.

The raw fractograms (UV absorbance at 270 nm, fluorescence at 350/450 nm (excitation/emission) or elemental

Table 2
Fractionation conditions and ICP-MS instrument operating parameters for flow FFF ICP-MS system

Flow FFF conditions:	
Channel dimensions (cm)	$26.0 \times 2.0 \times 0.0156$
Channel volume (mL)	0.81
Channel flow rate (mL min^{-1})	0.5 ± 0.01
Cross flow rate (mL min^{-1})	3.0 ± 0.1
Relaxation time (s)	60
UV wavelength (nm)	270
Fluorescence wavelengths (nm)	350/ 450
ICP-MS (Thermo Finnigan ELEMENT 1) instrument settings and operation parameters:	
RF generator frequency (MHz)	27
RF power (W)	1500 (variable)
Cool gas flow rate (L min^{-1})	15 (variable)
Auxiliary gas flow rate (L min^{-1})	1.0 (variable)
Sample gas flow rate (L min^{-1})	1.2 (variable)
Ion lens settings	Adjusted for maximum signal intensity
Torch	Fassel torch
Nebulizer	Burgener mira mist
Spray chamber	Scott type
Sample cone	Nickel, 1 mm orifice diameter
Skimmer cone	Nickel, 0.7 mm orifice diameter
Sample take-up rate (mL min^{-1})	1.0

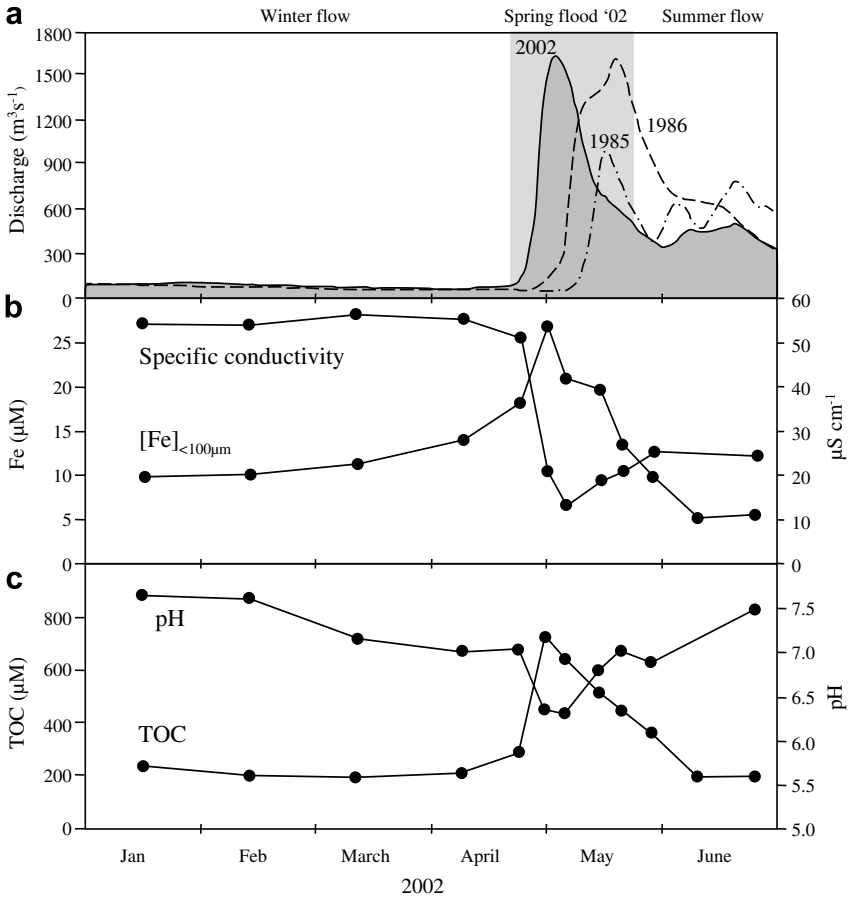

Fig. 1. Temporal variations in (a) discharge for 2002, 1986 and 1985, (b) [Fe] and specific conductivity, (c) TOC and pH, and (d) water temperature and sunlight. [Fe] and TOC indicate total concentrations of iron and organic carbon in prefiltered water.

concentration as a function of the retention time) were converted into frequency distributions against size or molecular weight. Size was estimated as the hydrodynamic diameter distribution as described in FlFFF theory (Hovingh et al., 1970; Beckett et al., 1987). Molecular weight was estimated by calibration with polystyrene sulfonate (PSS) standards.

All FlFFF carrier reagents used were of analytical grade dissolved in MQ water. Metal standards were prepared by dilution of 10 mg L^{-1} mixed standards (SPEX CertiPrep®, Glen Spectra Reference Materials, Stanmore, England) and spikes from dilution of 1000 mg L^{-1} stock standard solutions (Merck®). High purity acid was prepared in a clean laboratory by sub-boiling point quartz distillation of analytical grade HNO_3 (Merck®). The molecular weight standards used were polystyrene sulfonates (PSS) ranging from 1100 to 72,000 in molecular weight (Phenomenex®, Torrance, CA, USA) and dissolved in the carrier. These standards correspond approximately to a range of 1–12 nm in hydrodynamic diameter.

2.6. TOC

Prefiltered samples were also collected and analyzed for total organic carbon (TOC). The concentration was measured in all permeate and retentate fractions from the ultrafiltrations using a Shimadzu TOC-5000 high temperature catalytic oxidation instrument, with an accuracy of ±10%, (1 s.d.). Samples were acidified and sparged before analysis and potassium hydrogen phthalate was used as a standard substance.

3. RESULTS

3.1. Seasonal cycle of master variables

Fig. 1 summarises the changes in master variables in the Kalix River over the period January to June 2002. The most dramatic change occurs in the freshwater discharge, where the peak flow occurred unusually early in 2002, increasing

Fig. 2. FlFFF Fractograms for selected elements on sampling dates representing winter conditions (9 April), spring flood (1 May) and summer conditions (10 June). The *y*-axis scales are arbitrary, so that the fractograms shapes can be seen despite wide variations in concentration between elements and between sampling dates. The colloidal concentrations obtained by integrating these fractograms are shown in Table 4. The UV and fluorescence signals are shown separately for 9 April, where they differ significantly; on 1 May and 10 June they show the same size distribution, and only the UV signal is plotted.

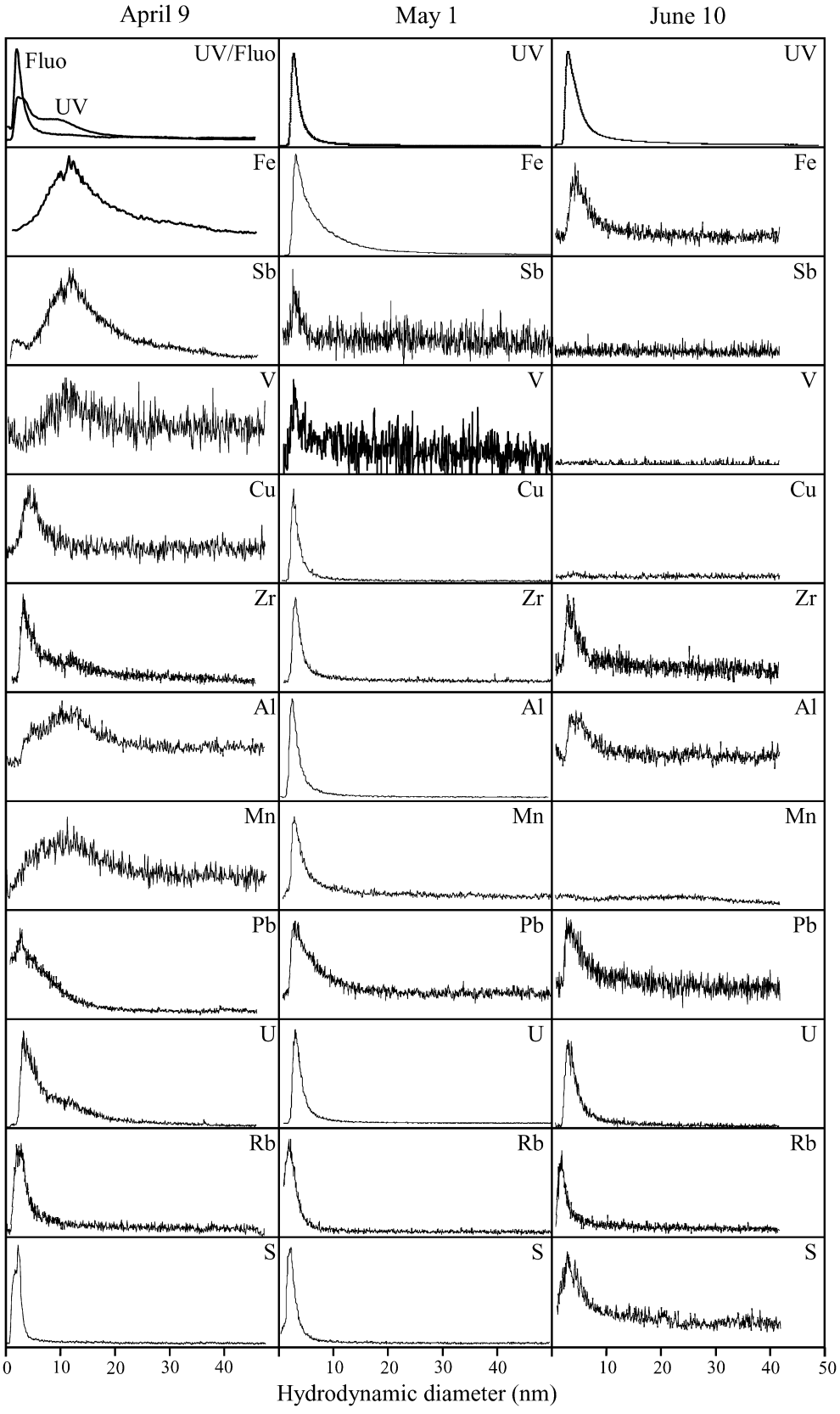
April 9
May 1
June 10
Fluo
UV
UV/Fluo
UV
UV
Fe
Fe
Fe
Sb
Sb
Sb
V
V
V
Cu
Cu
Cu
Zr
Zr
Zr
Al
Al
Al
Mn
Mn
Mn
Pb
Pb
Pb
U
U
U
Rb
Rb
Rb
S
S
S
0 10 20 30 40
10 20 30 40
10 20 30 40 50
Hydrodynamic diameter (nm)

by more than an order of magnitude within a period of one week (Fig. 1a). The dramatic discharge peak is accompanied by a drop in pH and in the concentrations of dissolved major ions (represented by specific conductivity in Fig. 1b) but increases in both iron and organic carbon concentrations. The spring flood is therefore associated with significant changes in the master variables controlling water chemistry. In addition, the post-spring flood master variables are in several cases significantly different to the winter values (e.g. specific conductivity and Fe concentration). For convenience, the three different chemical regimes shown in Fig. 1 (pre-flood, spring flood and post-flood) will be referred to as winter, spring and summer in this paper.

3.2. Seasonal cycle of small colloidal concentrations

Our investigation of the distribution and fractionation of the lanthanide elements during the same study (Andersson et al., 2006) showed that the colloidal material in the Kalix River is dominated by iron and carbon, which are considered to act as colloidal carrier phases. During winter flow separate iron and carbon carrier phases can be detected with FlFFF. However, during spring flood and summer flow iron is associated with the carbon carrier phase. The same colloidal carrier phases were identified in a study of colloidal chemistry in a small creek in southern Sweden (Lyvén et al., 2003). The difference between winter and spring/summer conditions has been further assessed by Ingri et al. (2006), who showed by measuring the iron isotopic composition that the two phases differ with up to 0.44‰ (δ^{56}Fe). Other elements in the colloidal fraction are considered to be associated with one or other of these carrier phases.

In the Kalix River, individual chemical elements associated with colloidal material show significant variations with respect to both colloidal size (hydrodynamic diameter) and season. In order to illustrate these variations, we have selected 10 elements representing contrasting behaviours, and have plotted their FlFFF fractograms for three sampling times representing winter (9 April), spring (1 May), and summer (10 June). These fractograms are shown in Fig. 2, while Table 3 provides summary information for all the elements studied. The different noise levels in these fractograms reflect in large part the widely varying colloidal concentrations of the individual elements, which are summarised in Table 4. Of the colloidal carrier phases, Fe is shown directly while C is represented indirectly as UV. The ~10 nm shoulder on the 9 April UV trace is the one clear difference between the UV and fluorescence fractograms, and appears to be related to the Fe fractogram peak in the same size range: the lack of fluorescence response suggests that either no significant humic component is present in this size range, or possibly that humic fluorescence is quenched. In spring and summer, when the colloidal material is dominated by organic carbon, UV and fluorescence show virtually identical fractograms. Fluorescence data will not be further discussed in this work, but will be the topic of a future article.

Of particular interest in Fig. 2 are the winter (April 9) data, where the Fe and C colloidal carriers show very different size distributions, allowing the association of different elements with these two carriers to be examined. We will return to this point later (Section 4), but will first look in more detail at the temporal sequence of elemental distributions, as revealed by the size fractionation studies.

3.3. Size fractionation of selected elements

Table 5 summarises the seasonal changes in prefiltered and 0.22 μm permeate concentrations of the elements studied, and selected elements are shown in more detail in Fig. 3. The majority of the trace elements show a clear maximum in prefiltered concentrations at the spring flood, the exception being Mo which shows a clear minimum indicative of Mo being diluted by the water discharge from snowmelt, following the behaviour of the major elements, e.g. Na, Ca, Mg, Cl and SO_4 noted in Section 3.1. Our analysis of lanthanide fractionation patterns (Andersson et al., 2006) led us to conclude that the lanthanide elements measured in the spring flood have an entirely different source to that in the winter and summer periods. The spring flood source, proposed as topsoil flushed by melt water and flooded riverside areas, is not rich in the major elements noted above, nor in Mo, since all of these are diluted by the intense water discharge. This is supported by Tyler (2005) who showed that major elements generally are not enriched, as in the case of the lantanide elements, but instead removed from the O-horizon. In contrast to Na, the heavier alkali metals (K, Rb, Cs) show maximum concentrations during the spring flood, consistent with these elements being retained in the topsoil, as observed in a different system by Tyler (2004). A general feature of the elemental size distributions shown in Fig. 3 is that variations in the 1 kDa permeate concentration over time are smaller than in the larger fractions. This is most clearly shown for Co, where the 1 kDa permeate is essentially constant while the larger fractions show a very well defined peak at the spring flood.

The results shown in Fig. 3 are drawn from two of the fractionation techniques used in this study: CFF and FlFFF (DGT is discussed in more detail in section 3.4 below) While there is a reasonable overall agreement as to the general trends, significant differences and/or discrepancies arise when a more quantitative comparison is attempted. Thus, comparison between CFF and FlFFF estimates of colloidal concentrations also reveal wide variations. Thus the two estimates agree well for Fe, while FlFFF gives very much lower values for Co and Rb. These differences may arise from the different physicochemical conditions employed in the two techniques (see discussion in Dahlqivst et al., 2004), and/or from the use of different 1 kDa membranes, which may have different effective cutoff values for natural complexes and colloids.

3.4. DGT

We have previously (Andersson et al., 2006) identified two problems associated with the quantitative interpreta-

Table 3
Seasonal overview of colloidal chemistry in the Kalix River 2002: (1) colloidal carrier phase for each element during winter (9 April data); (2) increase (+) or decrease (−) in colloidal concentration between winter (9 April) and spring (1 May); (3) timing of maximum in colloidal concentration

	(1)[a]	(2)	(3)
Main group elements			
Li	n.c.		
Na	n.c.		
K	n.c.		
Rb	n.c.		
Cs	C/Fe		
Be	n.d.		
Mg	C/Fe	+	Winter
Ca	C/Fe	+	Winter
Sr	C/Fe	+	Summer
Ba	C/Fe	+	Spring
B	n.d.		
Al	C/Fe	+	Spring
Ga	n.d.		
Tl	n.d.		
C	C		
Si	Fe		
Sn	n.d.		
Pb	C/Fe	+	Spring
P	Fe	−	Winter
As	n.d		
Sb	Fe	−	Winter
Bi	n.d.		
S	n.c.		
Se	n.d.		
Te	n.d.		
Cl	n.c.		
Br	n.d.		
I	C	+	Spring
Transition elements			
Sc	n.d.	+	Spring
Ti	n.d.		
V	Fe	+	Spring
Cr	C/Fe	+	Summer
Mn	C/Fe	+	Summer
Fe	Fe	−	Winter
Co	C	+	Spring
Ni	C	−	Spring
Cu	C	+	Spring
Zn	Fe	−	Winter
Y	C/Fe	+	Spring
Zr	C	+	Spring
Nb	n.d.		
Mo	n.c.		
Ag	n.d.		
Cd	n.d.		
Hf	C	+	
Ta	n.d.		
W	n.d.		
Re	n.d.		
Os	n.d.		
Pt	n.d.		
Au	n.d.		
Hg	n.d		
Lanthanides and actinides			
La	Fe	+	Spring
Ce	Fe	+	Spring
Pr	Fe	+	Spring
Nd	Fe	+	Spring
Sm	C/Fe	+	Spring
Eu	C/Fe	+	Spring
Gd	C/Fe	+	Spring
Tb	C/Fe	+	Spring
Dy	C/Fe	+	Spring
Ho	C/Fe	+	Spring
Er	C/Fe	+	Spring
Tm	C/Fe	+	Spring
Yb	C/Fe	+	Spring
Lu	C/Fe	+	Spring
Th	C/Fe	+	Spring
U	C/Fe	+	Spring

[a] "n.c." = not present in colloidal form; elements marked "n.d." = colloidal distribution cannot be distinguished from the background.

Table 4
Integrated colloidal concentrations (nM) for the fractograms shown in Fig. 2

Element	Winter (9 April)	Spring (1 May)	Summer (10 June)
Fe	1241 (8.8)	1159 (4.3)	3 (0.06)
Sb	1.46[a]	[b]	[b]
V	0.043[a]	0.269 (3.4)	[b]
Cu	0.6 (11.2)	3.5 (34.2)	0.4[a]
Zr	0.25[a]	1.24[a]	0.27[a]
Al	46 (8.1)	262 (10.7)	10 (1.8)
Mn	0.87 (0.4)	6.32 (0.7)	6.72 (2.2)
Pb	[b]	0.088 (46)	0.020 (13)
U	0.087[a]	0.108 (10.1)	0.024 (4.1)
Rb	0.144 (1.0)	0.206 (0.9)	0.147 (1.0)
S	324 (0.6)	405 (1.9)	340 (0.9)

Values in parantheis are % colloidal of the total concentration.
[a] Total concentration was not determined.
[b] Fractogram could not be integrated as the colloidal distribution could not be distinguished from the background.

tion of DGT data from this field campaign. First, the preparation (washing) procedure used in the work, and which was standard procedure for DGT measurements at that time, can lead to (up to 5-fold) accelerated diffusion of metal ions through the gel at low ionic strength, resulting in an underestimate of labile metal concentrations calculated according to Equation 1 (Warnken et al., 2005). "Low ionic strength" in this context is <1 mM: calculated ionic strengths for the Kalix samples range between 0.3 and 0.7 mM, the lowest values occurring at the spring flood. Second, complexation of metals by humic substances results in reduced diffusion coefficients (metal-fulvic acid complexes have typically a diffusion coefficient only 20% of that of the free metal ion; Scally et al., 2006). Since these two effects oppose one another, but cannot be fully quantified, we can most safely report the DGT measurements in terms of the most probable range of concentrations of DGT-labile metal. In order to assess this range we have first estimated the reduction in diffusion coefficient due to com-

Table 5
Spring flood characteristics of elemental concentrations in the Kalix River 2002

	Prefiltered	0.22 μm permeate
Main group elements		
Li	No	No
Na	Min	Min
K	Max	No
Rb	Max	Max
Cs	Max	No
Be	No	No
Mg	Min	Min
Ca	Min	Min
Sr	Min	Min
Ba	No	Min
B		
Al	Max	Max
Ga	Max	Max
Tl	No	Max
C	Max	Max
Si	Min	No
Sn		
Pb	Max	No
P	Max	Local max
As	No	No
Sb	No	No
Bi		
S	Min	Min
Se		
Te		
Cl		
Br		
I		
Transition elements		
Sc	No	Max
Ti	Max	Local max
V	Max	Local max
Cr	Max	No
Mn	Max	Max
Fe	Max	Local max
Co	Max	Max
Ni	Max	No
Cu	Max	No
Zn	Local max	No
Y	Max	Local max
Zr	No	No
Nb	No	No
Mo	Min	Min
Ag		
Cd	No	No
Hf	No	No
Ta		
W	No	No
Re	No	No
Os		
Pt	No	No
Au	No	No
Hg	No	
Lanthanides and actinides		
La	Max	Local max
Ce	Max	Local max
Pr	Max	Local max
Nd	Max	No
Sm	Max	Local max
Eu	Max	No
Gd	Max	Local max
Tb	Max	No
Dy	Max	Local max
Ho	Max	No
Er	Max	Local max
Tm	Max	No
Yb	Max	Local max
Lu	Max	No
Th	No	No
U	No	No

plexation with humic materials, and then considered that the diffusion coefficient may in reality be between 1 and 5 times this corrected coefficient depending on the strength of the acceleration effect. In the case of the lanthanides, these elements were estimated from speciation calculations to be essentially 100% complexed by humic materials. Since the range of metals being considered in the paper shows a much wider range of behaviour, the degree of humic substance complexation of the metals measured by DGT was calculated for each of the sampling occasions, with the overall results shown in Table 6. Since these discrete samples do not coincide with the DGT deployment periods, the mean degree of complexation has been used in calculating the probable ranges of DGT-labile metal concentrations shown in Fig. 4. For Fe, Mn, Al, Ni and Co, the 0.2 μm permeate concentrations fall largely within these calculated DGT-labile concentration ranges, suggesting that DGT is sampling essentially all of the 0.2 μm permeate, with the notable exception of Fe during the winter season, where the DGT system appears to sample only a small proportion of the 0.2 μm permeable Fe. This may indicate the existence of colloidal Fe, which is not DGT-labile. Co and Ni also show signs that DGT undersamples the 0.2 μm permeate during the winter season, suggesting that these metals may be associated with the non-labile Fe colloids. For Rb, the DGT-sampled concentrations are much less than the 0.2 μm permeate concentrations, reflecting the poor ability of the DGT resin to complex and accumulate the weakly interacting Rb^+ ion.

4. DISCUSSION

Figs. 2 and 3 demonstrate that colloidal material plays a significant role in the transport of trace metals in the Kalix River. The seasonal behaviour of each element can be characterised by the answers to the following questions.

- Is the "dissolved" (0.22 μm permeate) concentration at the time of the spring flood a maximum value (indicating that the flood water has been enriched in this element), or a minimum value (indicating that the flood water is acting to dilute out this element)?

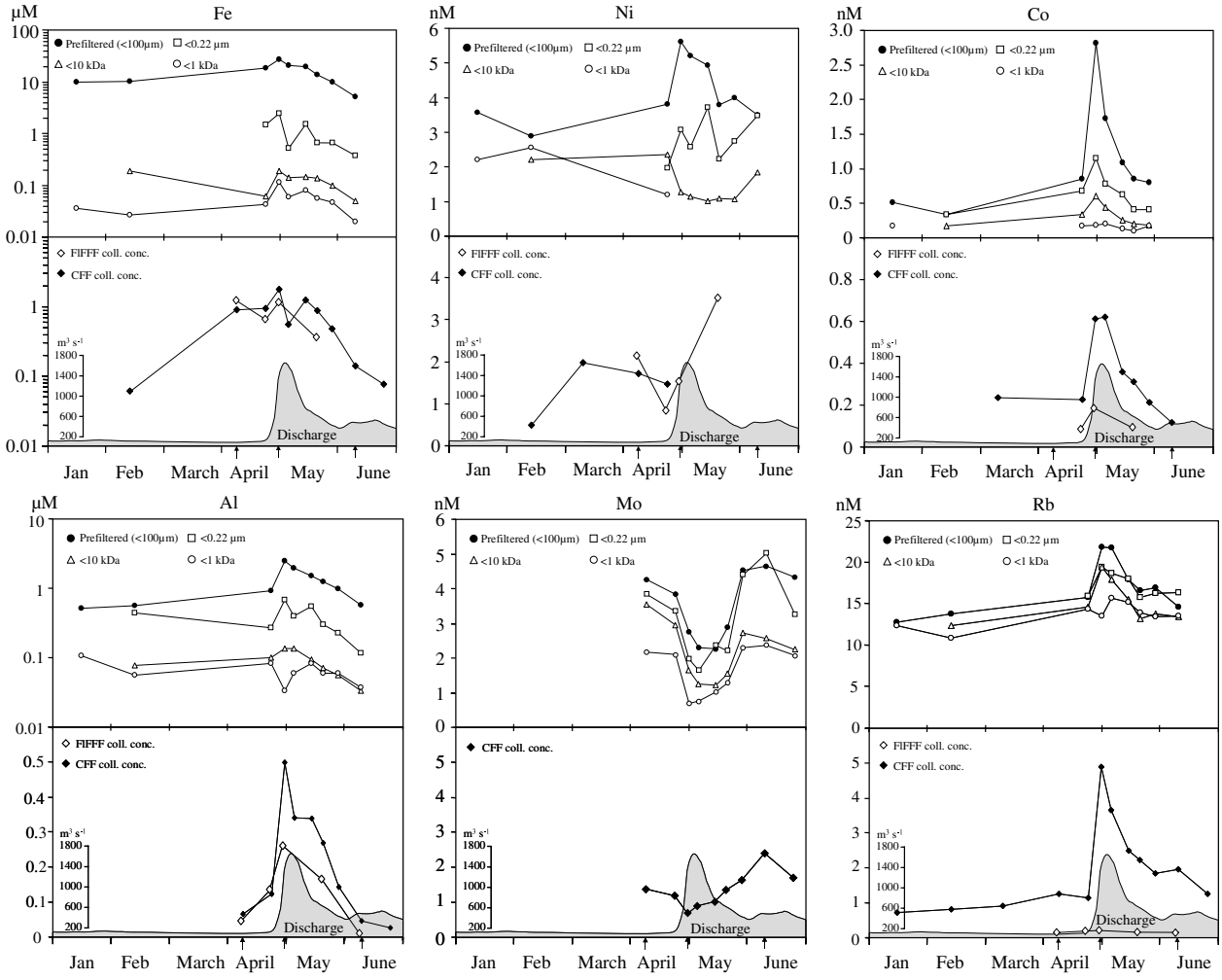

Fig. 3. Concentrations of Fe, Ni, Al, Mo and Rb in different size fractions in the Kalix River between January and June 2002. Note that the concentration scale for Fe is logarithmic.

Table 6
Calculations of complexation in the Kalix field samples

Element	% Bound by humic substances[a]
Mg	6.3 ± 3.8
Al	100
Ca	7.2 ± 4.0
Mn	35.7 ± 7.7
Fe	99.3 ± 0.4
Co	35.3 ± 12.2
Ni	59.7 ± 12.4
Sr	16.1 ± 7.5
Ba	3.8 ± 2.4
U	92.2 ± 3.5

[a] Calculated using the speciation programme WHAM 6.

- Does the element associate preferentially with the iron or the carbon colloidal carrier phase?
- Does the colloidal concentration of the element show a maximum during the winter, or during the spring or summer?

By answering these three questions we can in more detail draw conclusions on the association of trace elements to certain colloidal carrier phases and link these to the discussion of hydro-geological residence times and pathways for soil and ground water.

Tables 3 and 5 summarise this information for all the elements studied in the "Kalix 2002" project. Several elements included in the measurement programme could not be quantified since the colloidal size distributions could not be distinguished from the background: these are however included in these Tables for completeness. The relative degree of association with Fe and C colloidal carrier phases has been assessed from the 9 April fractograms, and as for the fractograms shown in Fig. 2 have been divided into three categories: Fe-dominated, C-dominated and mixed. The elements whose distribution is dominated by truly dissolved material are marked as "n.c." (non-colloidal) in Table 3. The distributions of the lanthanide elements have been addressed in a separate paper (Andersson et al., 2006), and will not be discussed further here. Table 3 also shows the timing of the maximum in col-

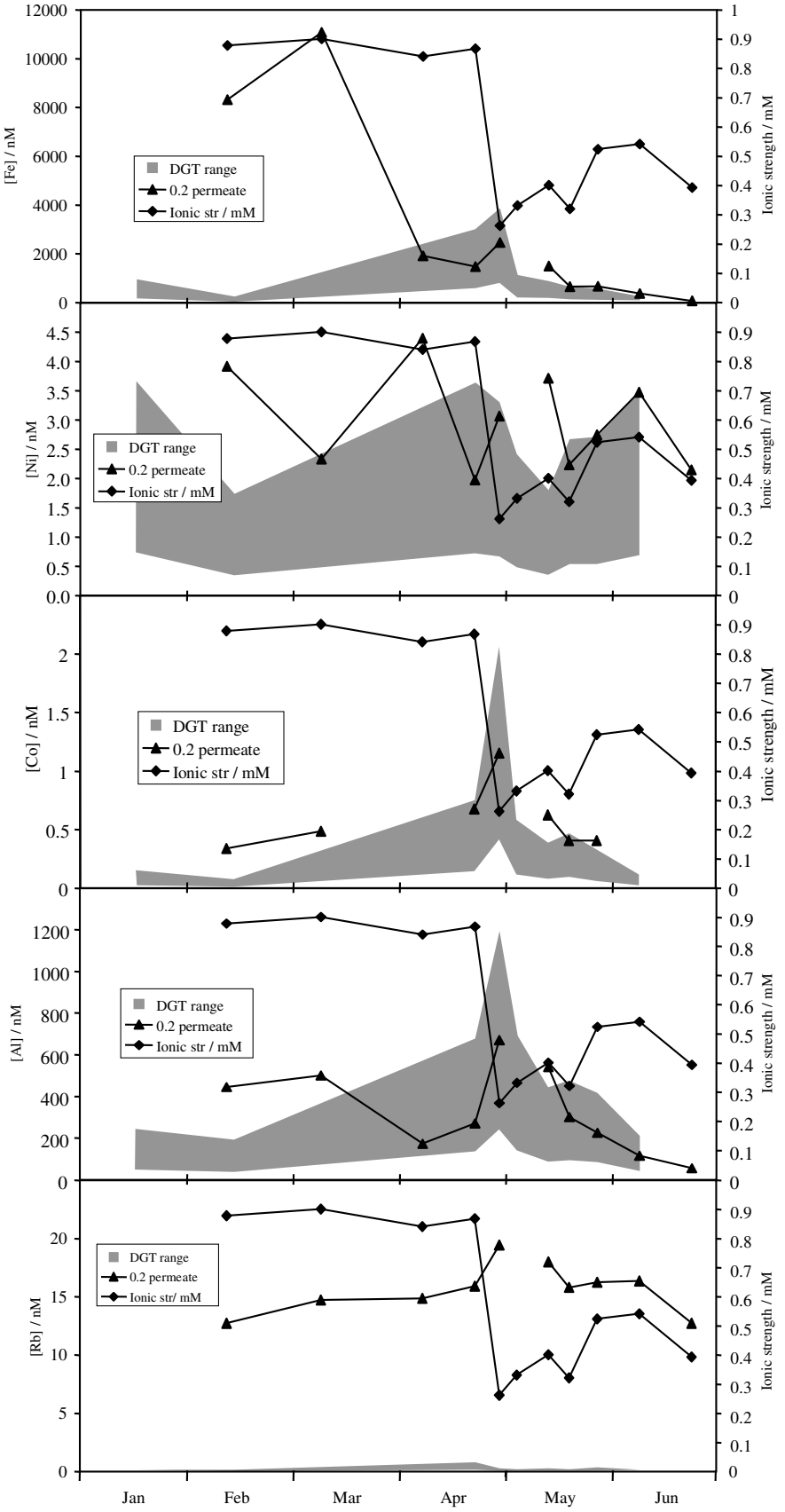

Fig. 4. DGT-labile concentration ranges for Fe, Ni, Co, Al and Rb calculated as described in Section 3.4. The 0.22 μm permeate concentrations of these elements are also shown, together with the calculated ionic strength of the water samples.

loidal concentration of each element. The elements associating strongly with the Fe colloidal carrier phase show a maximum in the winter, their colloidal concentrations declining thereafter as the carrier phase concentration decreases. The majority of the remaining elements, whether strongly C-associated or associated with both colloidal carrier phases, show a maximum during the spring period. Analysis of the lanthanide fractionation patterns from the same sampling occasions has indicated that the source of colloidal lanthanides, and by implication also the source of the colloidal carrier phases, varies according to season, with mobilised organic material from flooded topsoil considered to play an important role during the spring flood (Andersson et al., 2006).

4.1. Association with colloidal carrier phases

The presence of two colloidal carrier phases has previously been reported in the Kalix River by Dahlqivst et al. (2004) and Andersson et al. (2006). However, their origin and temporal variation in relation to geochemical processes in soil and ground water have not been discussed in detail. In short, two colloidal particles with different chemical composition and size have been observed in the river; a smaller (~2–3 nm) organic-rich colloid, and a larger (~12 nm) Fe-rich particle. The temporal variation of these colloids leads us to be believe that the relative significance of different hydro-geological pathways change during the year. We propose that the larger Fe-rich colloid observed only during winter conditions has its origin in deep ground waters with long residence times. The long residence time for ground water during winter is facilitated by the fact that precipitation is accumulation as snow instead of acting as input to the groundwater reservoir. Effectively, this gives the groundwater longer time to interact with its surrounding bedrock. This is supported by recent findings in the Kalix River by Ingri et al. (2006), where it was suggested that Fe-oxyhydroxides are precipitated during winter by inflow of oxygen deficient groundwater enriched in Fe(II). Furthermore, the steady and increasing concentration of suspended Fe-oxyhydroxides observed during winter by Ingri et al. (2006) was responsible for an increase in δ^{56}Fe by approximately 0.4‰.

Although the smaller C-rich colloidal fraction also can be observed during winter it seem that Fe is not associated with this material, at least not to a degree which is detectable with our equipment. However, as the spring flood event starts the large Fe-oxyhydroxides can no longer be detected, and Fe is instead associated with the C-rich colloidal matter.

The small sized organic colloidal material probably has its origin in the uppermost organic-rich soil layer (O-horizon) in the podzol. Normally, most of the organic material is percolated down through the soil horizons and subsequently precipitated together with Fe and Al in the B-horizon (podzolisation). However, during snowmelt in spring the uppermost layers can be intensively flushed, and organic material can be readily mobilized and reach surface waters without being precipitated in the B-horizon. Along with the organic material are associated Fe, Al and other trace elements.

The overview of carrier phase association presented in column (1) of Table 3 is compared in Fig. 5 with the earlier FlFFF-ICP-MS study of trace element distribution between Fe and C colloidal carrier phases in the small Delsjö Creek in southern Sweden (Lyvén et al., 2003). The elements dominated by C-colloids in the Kalix river are also C-dominated in the Delsjö Creek, while the majority of elements display en intermediate behaviour in both systems. However, two elements (Pb and Sb) depart from this pattern showing sharply contrasting behaviour in the two systems. We can conclude that these two elements' behaviour are strongly dependent on the chemistry of the water and/or colloids: pH may well play a significant role here, since the speciation modelling study reported by Lyvén et al. (2003) suggests that the distribution of Pb between Fe and C colloids may be strongly pH-dependent.

An interesting aspect of the overview shown in Table 4 concerns the elements with potentially variable oxidation states, where the observed fractionation can provide an indication of the oxidation state of the elements concerned. The case of V is discussed in Section 4.1.1: Cr is also interesting in this connection. Cr can be present as Cr(III) or Cr(VI) in natural waters. Of these, Cr(VI) as chromate is expected to be dominated by truly dissolved material as for the isostructural sulphate and molybdate. The observation that Cr is associated with both C and Fe colloidal carrier phases is therefore not consistent with the presence of Cr(VI): on the other hand, association with both C and Fe colloidal carrier phases is fully consistent with the presence of Cr(III) (cf. other trivalent cations such as Al and the heavier lanthanides).

4.1.1. Strong association with fe carrier phase

Sb and V are the representative elements in this case. Both elements are clearly associated with the Fe peak under winter conditions (9 April), and together with Fe show very low or undetectable colloidal concentrations in summer (Fig. 2 and Table 3). The strong association of V with Fe colloids suggests that V is present as the thermodynamically favoured

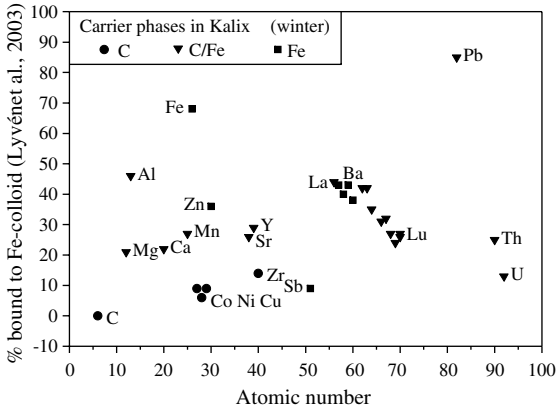

Fig. 5. Comparison of the major carrier phases of the elements in the Delsjö Creek (Lyvén et al., 2003) and the Kalix River (this work). The Delsjö data are expressed as a percentage derived from a deconvolution analysis, while the Kalix data are divided into the three categories shown in column (1) of Table 4.

oxidation state V(V), whose oxyanions are isostructural with phosphate. Phosphate is well known to associate strongly with iron oxide surfaces, and was also clearly associated with the Fe colloidal carrier phase on 9 April, although the P fractograms were very noisy. Since V is not associated to any colloidal phase during summer it is likely that the origin for V during winter also, like Fe, is from groundwater supply. However from our data it can not be deduced for certain if V binds to the Fe-colloids during an early stage of precipitation, or is adsorbed at a later stage when the colloids have already reached the river.

Little is known of Sb speciation in river waters, but the strong association with Fe suggests a similar mechanism of strong anion adsorption to the iron oxide surface. Association of Sb and V to carbon colloids is on the other hand very weak, which most probably reflects the weak interaction of anions with the negatively charged humic substances, which constitute a significant part of the organic carbon present.

4.1.2. Strong association with C carrier phase

Zr and Cu are the representative elements in this case. The colloidal concentrations follow carbon, showing a clear maximum in colloidal concentration at the spring flood, while association with Fe colloids is too weak to be identified in the 9 April fractograms. These two elements represent very different chemistries. The association of the strongly hydrolysed Zr(IV) with organic carbon parallels the well-known strong uptake of the analogous Th(IV) by biogenic organic matter in the ocean, a process which forms the basis for estimation of vertical particulate fluxes using U - Th disequilibria measurements as suggested by Turekian (1977). Like Zr and Th, Hf also falls within this group showing strong association with the C-colloid and increasing concentration during the spring flood. The work of Tyler (2005) shows moderate enrichment of Zr, Th and Hf in the O-horizon, which agree with our findings. Cu(II), with a very different chemistry as a ''borderline'' cation (i.e. intermediate between (a)- and (b)-type cations) is also well known to form strong organic complexes, and can therefore be expected to associate strongly with organic carbon colloids. Thus, it is possible for carbon-rich colloidal material to act as a strong 'scavenger' for some trace elements (e.g. Th, Zr, Hf), but also as a surface with continuous adsoption and exchange with solute species in the surrounding water.

As C-rich colloids likely derive from the uppermost soil horizon it is also likely that many of the trace elements associated with this carrier phase (e.g. Co, Ni, Cu) have their origin here. In a study on vertical trace element distribution in a Haplic Podzol profile, in southern Sweden, it was shown by Tyler (2004) that there was a strong correlation between organic matter and many transition elements, including Co, Ni, Cu, Pb and Zn. It is also consistent with our findings that organic colloidal matter is enriched in these elements in the river water during snowmelt and spring flood.

4.1.3. Association with both carrier phases

Many elements associate with both the Fe and C colloidal carrier phases: this is most clearly shown by the fractograms for 9 April where the Fe and C colloidal carrier phases show very different size distributions. Al, Mn, Pb and U represent this grouping in Fig. 2. This group of elements combines contrasting chemistries including strongly hydrolysed (Al) and weakly hydrolysed (Pb) cations, and elements with potentially variable oxidation states (Mn, U).

4.2. Truly dissolved elements

Elements that are largely present in truly dissolved form show fractograms dominated by a ''void peak'', i.e. a peak which occurs at a shorter retention time than either of the colloidal carrier phases. This ''void peak'' is interpreted as a flushing of truly dissolved material from the FlFFF channel, and is not considered to represent colloidal material. Rb and S are the two such elements shown in Fig. 2. In terms of chemistry, we can note that Rb, in common with other alkali metal cations, interacts only very weakly with ligands and particulate material (with the exception of clays), so that a distribution dominated by truly dissolved material is not unexpected. S is present as the anion sulphate, which can be expected to interact only very weakly with negatively charged organic carbon colloids (c.f. discussion of vanadate in Section 4.1.1 above), and in contrast to V does not interact significantly with iron oxide surface either.

5. CONCLUSIONS

The intense spring flood in the Kalix River is accompanied by major changes in the dissolved, colloidal and particulate concentrations of major and trace elements. The colloidal material is dominated by carbon and iron colloids, which are considered to act as carrier phases for other elements. Iron is the dominating colloidal carrier phase in winter, giving way to carbon during the spring flood. Consequently, this behaviour results in significant changes in the colloidal concentrations of many trace elements, most particularly those that have a particularly strong affinity for one or other of the two carrier phases. Elements that associate with the carbon colloidal carrier phase show a strong maximum in colloidal concentration at the time of the spring flood. The alkali metals, together with many oxyanionic elements, associate only very weakly with colloidal carrier phases and occur largely as truly dissolved material. Important exceptions are elements such as V and Sb, which have a strong affinity for the iron colloidal carrier phase. Thus, the nature of the colloidal carrier phases, and elemental affinities for these, strongly influence the colloidal transport of elements in the Kalix River.

The cause for these changes in colloidal concentrations, and associated trace elements is attributed to variations in hydro-geological pathways, which seem to be dramatically variable during spring flood. Winter conditions promote formation of Fe-colloids when oxygen deficient groundwater enters the river. Due to accumulation of snow during winter the ground water has a long residence time compared to summer conditions. It is therefore enriched in Fe(II), which precipitates to form a Fe-oxyhydroxide col-

loidal phase to which other trace elements are associated. At peak spring flood the hydro-geological conditions are different. A combination of rapid snowmelt and/or flooded riverbanks cause the uppermost organic-rich soil layer to be washed. As a result organic matter, including colloidal particles, is mobilised and carried to the river during this period, and the Fe-rich colloid can not be observed Summer conditions provide yet another regime for river geochemistry. Precipitation not returned to the atmosphere by evapo-transpiration readily percolates to the groundwater reservoir, receiving the geochemical imprint of the physical and chemical characteristics of the soil profile and bedrock. Intense storm events during summer are likely to simulate similar conditions as observed during snowmelt and spring flood.

Three independent techniques for physico-chemical speciation have been used to characterise the size fractionation of the elements studied. While the trends shown by these techniques are largely consistent with one another, quantitative comparisons reveal some important differences that warrant further investigation.

We conclude that river geochemistry is controlled by a combination of hydro-geological pathways and geological conditions in soil and bedrock. The colloidal speciation and concentration, with associated trace elements, are closely linked with these processes. Climate is a major aspect in controlling hydrogeology in boreal and arctic regions. Type, duration and intensity of precipitation are probably key factors. As with many rivers in high-latitude regions discharge is highly variable, and the physico-chemical speciation may change accordingly as has been proven in the Kalix River.

We have analysed 42 trace elements in the size range from 'truly dissolved' elements to particulate material <100 μm in an attempt to give a detailed account of the temporal variation in physico-chemical speciation. Colloidal particles are important carriers for trace elements. Thus, we have elaborated on the origin and evolution of colloidal particles in the Kalix River and how these receive the observed geochemical imprint from interaction between soil, bedrock, water and particles and solute species transported therein.

ACKNOWLEDGMENTS

The authors would like to thank Anders Henriksson, Johan Gelting-Nyström, Helena Skoglund and Jerry Forsberg at Luleå University of Tech. for their assistance during collection and processing of samples. We are grateful to Rickard Hernell and Ilia Rodushkin at Analytica Corp. for help during sample preparation, analysis and setup of the MS used for FlFFF. We thank Hao Zhang for fruitful discussions on the interpretation of DGT results.

This work is supported by Swedish Research Council Grants G 5103-20005567/2000 (D.T.) and G-AA/GU 640-2645/1999 (J.I.).

We thank Jens Hölemann and an anonymous reviewer for providing helpful suggestions for improving the manuscript.

REFERENCES

Allard T., Menguy N., Salomon J., Calligaro T., Weber T., Calas G. and Benedetti M. F. (2004) Revealing forms of iron in river-borne material from major tropical rivers of the Amazon Basin (Brazil). *Geochim. Cosmochim. Acta* **68**, 3079–3094.

Andersson K., Dahlqvist R., Turner D., Stolpe B., Larsson T., Ingri J. and Andersson P. S. (2006) Colloidal rare earth elements in a boreal river: changing sources and distributions during the spring flood. *Geochim. Cosmochim. Acta* **70**, 3261–3274.

Andersson P. S., Porcelli D., Wasserburg G. J. and Ingri J. (1998) Particle transport of 234U–238U in the Kalix River and the Baltic Sea. *Geochim. Cosmochim. Acta* **62**, 385–392.

Andersson P. S., Dahlqvist R., Ingri J. and Gustafsson Ö. (2001) The isotopic composition of Nd in a boreal river: a reflection of selective weathering and colloidal transport. *Geochim. Cosmochim. Acta* **65**, 521–527.

Arnborg L., Walker H. J. and Peippo J. (1967) Suspended load in the Colville River, Alaska, 1962. *Geogr. Ann.* **49A**, 131–144.

Beckett R., Jue Z. and Giddings J. C. (1987) Determination of molecular weight distributions of fulvic and humic acids using flow field-flow fractionation. *Environ. Sci. Technol.* **21**, 289–295.

Benner R. (1991) Ultra-filtration for the concentration of bacteria, viruses and dissolved organic matter. In: Marine particles: Analysis and Characterisation (eds. D. C. Hurd and D. W. Spencer). Am. Geophys. Union, Washington, DC, Geophys. Monogr., 63, pp. 275–280.

Botch M. S., Kobak K. I., Vinson T. S. and Kolchugina T. P. (1995) Carbon pools and accumulation in peatlands of the former Soviet-Union. *Global Biogeochem. Cycles* **9**, 37–46.

Buffle J., Wilkinson K. J., Stoll S., Filella M. and Zhang J. (1998) A generalized description of aquatic colloidal interactions: the three-colloidal approach. *Environ. Sci. Technol.* **32**, 2887–2899.

Dahlqvist R., Zhang H., Ingri J. and Davison W. (2002) Performance of the diffusive gradients in thin films technique for measuring Ca and Mg in freshwater. *Anal. Chim. Acta* **460**, 247–256.

Dahlqvist R., Benedetti M., Andersson K., Turner D., Larsson T., Stolpe B. and Ingri J. (2004) Association of calcium with colloidal particles and speciation of calcium in the Kalix and Amazon rivers. *Geochim. Cosmochim. Acta* **68**, 4059–4075.

Dahlqvist R., Andersson P. and Ingri J. (2005) The concentration and isotopic composition of diffusible Nd in fresh and marine waters. *Earth Planet. Sci. Lett.* **233**, 9–16.

Davison W. and Zhang H. (1994) In situ speciation measurements of trace components in natural waters using thin-film gels. *Nature* **367**, 546–548.

Davison W., Fones G., Harper M., Teasdale P. and Zhang H. (2000) Dialysis, DET and DGT: In situ diffusional techniques for studying water, sediments and soils. In *In situ Monitoring of Aquatic Systems: Chemical Analysis and Speciation* (eds. J. Buffle and G. Horvai). John Wiley, New York, pp. 459–569.

Dynesius M. and Nilsson C. (1994) Fragmentation and flow regulation of river systems in the northern third of the world. *Science* **266**, 753–762.

Fromm E. (1965) Beskrivning till jordartskartan över Norrbottens län, nedanför Lappmarksgränsen. SGU Serie Ca 39, 1–236. (In Swedish with English summary).

Gaal G. and Gorbatschev R. (1987) An outline of the Precambrian evolution of the Baltic Shield. *Precambrian Res.* **35**, 15–52.

Gee D. G. and Zachrisson E. (1979) The Caledonides in Sweden. *SGU Ser. C.* **796**, 1–48.

Giddings J. C., Yank F. J. and Myers M. N. (1976) Theoretical and experimental characterization of flow field-flow fractionation. *Anal. Chem.* **48**, 1126.

Gordeev V. V., Martin J. M., Sidorov I. S. and Sidorova M. V. (1996) A reassessment of the Eurasian input of water, sediment, major elements, and nutrients to the Arctic Ocean. *Am. J. Sci.* **296**, 664–691.

Guo L., Hunt B. J. and Santschi P. H. (2001) Ultrafiltration behavior of major ions (Na, Ca, Mg, F, Cl, and SO_4) in natural waters. *Water Res.* **35**, 1500–1508.

Gustafsson &Ouml and Gschwend P. M. (1997) Aquatic colloids: concepts, definitions, and current challenges. *Limnol. Oceanogr.* **42**, 519–528.

Hassellöv M., Lyvén B., Haraldsson C. and Sirinawin W. (1999) Determination of continuous size and trace element distribution of colloidal material in natural water by on-line coupling of flow field-flow fractionation with ICP-MS. *Anal. Chem.* **71**, 3497–3520.

Hovingh E., Thompson G. H. and Giddings J. C. (1970) Column parameters in thermal field-flow fractionation. *Anal. Chem.* **42**, 195–203.

Ingri J. and Widerlund A. (1994) Uptake of alkali and alkaline-earth elements on suspended iron and manganese in the Kalix River, northern Sweden. *Geochim. Cosmochim. Acta* **58**, 5433–5442.

Ingri J., Torssander P., Andersson P. S., Mörth C-M. and Kusakabe M. (1997) Hydrogeochemistry of sulfur isotopes in the Kalix River catchment, northern Sweden. *Appl. Geochem.* **12**, 483–496.

Ingri J., Widerlund A., Land M., Gustafsson &Ouml, Andersson P. S. and Öhlander B. (2000) Temporal variations in the fractionation of the rare earth elements in a boreal river; the role of colloidal particles. *Chem. Geol.* **166**, 23–45.

Ingri J., Widerlund A. and Land M. (2005) Geochemistry of major elements in a pristine boreal river system; hydrological compartments and flow paths. *Aquat. Geochem.* **11**, 57–88.

Ingri J., Malinovsky D., Rodushkin I., Baxter D. C., Widerlund A., Andersson P., Gustafsson Ö., Forsling W. and Öhlander B. (2006) Iron isotope fractionation in river colloidal matter. *Earth Planet. Sci. Lett.* **245**, 792–798.

Land M. and Öhlander B. (1997) Seasonal variations in the geochemistry of shallow groundwater hosted in granitic till. *Chem. Geol.* **143**, 205–216.

Land M., Ingri J. and Öhlander B. (1999) Past and present weathering rates in northern Sweden. *Appl. Geochem.* **14**, 761–774.

Land M., Ingri J. and Öhlander B. (2000a) Chemical weathering rates, erosion rates and mobility of major and trace elements in a boreal granitic till. *Aquat. Geochem.* **6**, 435–460.

Land M., Ingri J., Andersson P. S. and Öhlander B. (2000b) Ba/Sr, Ca/Sr and 87Sr/86Sr ratios in soil water and groundwater: implications for relative contributions to stream water discharge. *Appl. Geochem.* **15**, 311–325.

Long S. E., and Martin T. D. (1990) Method 2008 determination of trace elements in waters and wastes by inductively coupled plasma: mass spectrometry, Technical Report Revision 4.4. Environmental Monitoring Systems Laboratory, U.S. Environmental Protection Agency, Cincinnati, Ohio.

Lyvén B., Hassellöv M., Haraldsson C. and Turner D. R. (1997) Optimisation of on-channel preconcentration in flow field-flow fractionation for the determination of size distributions of low molecular weight colloidal material in natural waters. *Anal. Chim. Acta* **357**, 187–196.

Lyvén B., Hassellöv M., Turner D., Haraldsson C. and Andersson K. (2003) Competition between iron- and carbon-based colloidal carriers for trace metals in a freshwater assessed using flow field-flow fractionation coupled to ICPMS. *Geochim. Cosmochim. Acta* **67**, 3791–3802.

Neff J. C., Finlay J. C., Zimov S. A., Davydov S. P., Carrasco J. J., Schuur E. A. G. and Davydova A. I. (2006) Seasonal changes in the age and structure of dissolved organic carbon in Siberian rivers and streams. *Geophys. Res. Lett.* **33**, L23401. doi:10.1029/2006GL028222.

Öhlander B., Ingri J., and Pontér C. (1991) Geochemistry of till weathering in the Kalix River watershed, northern Sweden. Reports from a Nordic Seminar, Uppsala 1991. Rep. 63. Swedish University of Agricultural Sciences.

Öhlander B., Land M., Ingri J. and Widerlund A. (1996) Mobility of rare earth elements during weathering of till in northern Sweden. *Appl. Geochem.* **11**, 93–99.

Öhlander B., Ingri J., Land M. and Schöberg H. (2000) Change of Sm–Nd isotope composition during weathering of till. *Geochim. Cosmochim. Acta* **64**, 813–820.

Pontér C., Ingri J., Burman J.-O. and Boström K. (1990) Temporal variations in dissolved and suspended iron and manganese in the Kalix River, northern Sweden. *Chem. Geol.* **81**, 121–131.

Pokrovsky O. S., Schott J. and Dupré B. (2006) Trace element fractionation and transport in boreal rivers and soil porewaters of permafrost-dominated basaltic terrain in Central Siberia. *Geochim. Cosmochim. Acta* **70**, 3239–3260.

Porcelli D., Andersson P. S., Wasserburg G. J., Ingri J. and Baskaran M. (1997) The importance of colloids and mires for the transport of uranium isotopes through the Kalix River watershed and Baltic Sea. *Geochim. Cosmochim. Acta* **61**, 4095–4113.

Post W. M., Emanuel W. R., Zinke P. J. and Stangenberger A. G. (1982) Soil carbon pools and world life zones. *Nature* **298**, 156–159.

Rember R. and Trefry J. (2004) Increased concentrations of dissolved trace metals and organic carbon during snowmelt in rivers of the Alaskan Arctic. *Geochim. Cosmochim. Acta* **68**, 477–489.

Scally S., Davison W. and Zhang H. (2006) Diffusion coefficients of metals and metal complexes in hydrogels used in diffusive gradients in thin films. *Anal. Chim. Acta* **558**, 222–229.

Stolpe B., Hassellöv M., Andersson K. and Turner D. (2005) High resolution ICPMS as an on-line detector for flow field-flow fractionation; multi-element determination of colloidal size distributions in a natural water sample. *Anal. Chim. Acta* **535**, 109–121.

Turekian K. (1977) The fate of metals in the ocean. *Geochim. Cosmochim. Acta* **41**, 1139–1144.

Tyler G. (2004) Vertical distribution of major, minor, and rare elements in a Haplic Podzol. *Geoderma* **119**, 277–290.

Tyler G. (2005) Changes in the concentration of major, minor and rare-earth elements during leaf senescence and decomposition in a Fagus Sylvatica forest. *Forest Ecol. Manag.* **206**, 167–177.

Vanýsek P. (2005) Ionic conductivity and diffusion at infinite dilution, In *CRC Handbook of Chemistry and Physics 85th ed.* (ed. D. R. Lide). CRC Press, Boca Raton, FL, pp. 5-76–5-78.

Viers J., Dupré B., Polvé M., Schott J., Dandurand J.-L. and Braun J.-J. (1997) Chemical weathering in the drainage basin of a tropical watershed (Nsimi-Zoetele site, Cameroon): comparison between organic-poor and organic-rich waters. *Chem. Geol.* **140**, 181–206.

Warnken K. W., Zhang H. and Davison W. (2005) Trace metal measurements in low ionic strength synthetic solutions by diffusive gradients in thin films. *Anal. Chem.* **77**, 5440–5446.

Associate editor: Johnson R. Haas